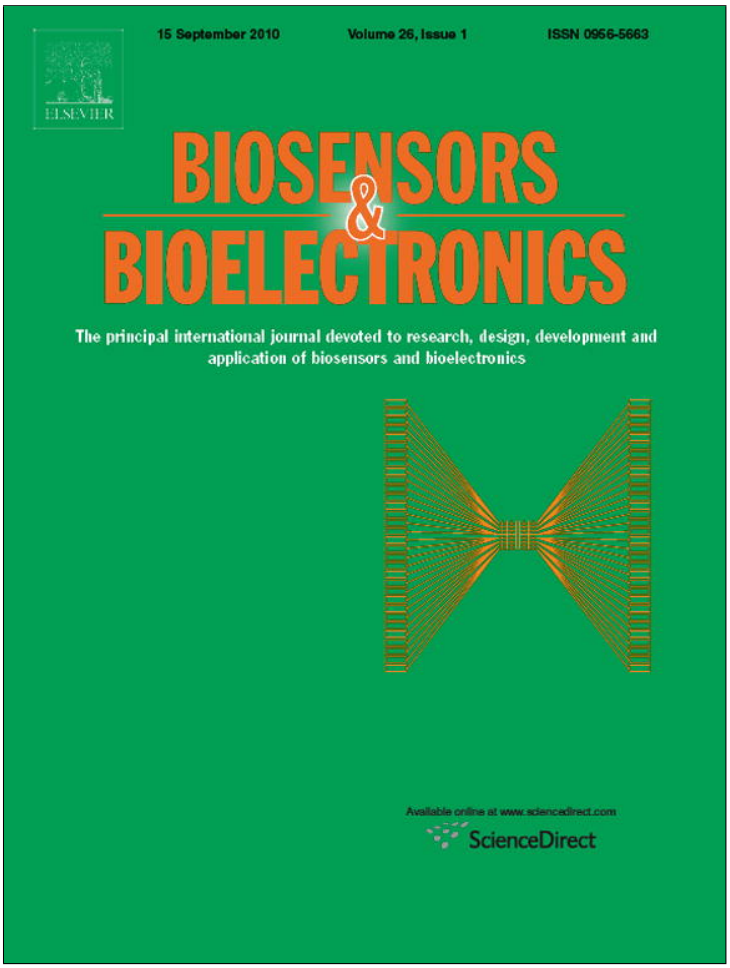

Report Documentation Page

Form Approved
OMB No. 0704-0188

1. REPORT DATE	2. REPORT TYPE	3. DATES COVERED
07 MAY 2010		

4. TITLE AND SUBTITLE	5a. CONTRACT NUMBER
Theophylline detection using an aptamer and DNA-gold nanoparticle conjugates	5b. GRANT NUMBER
	5c. PROGRAM ELEMENT NUMBER
6. AUTHOR(S)	5d. PROJECT NUMBER
	5e. TASK NUMBER
	5f. WORK UNIT NUMBER
7. PERFORMING ORGANIZATION NAME(S) AND ADDRESS(ES)	8. PERFORMING ORGANIZATION REPORT NUMBER
711 HPW/RHPC,2729 R Street,Bldg. 837 Area B,Wright-Patterson AFB ,OH,45433-5707	
9. SPONSORING/MONITORING AGENCY NAME(S) AND ADDRESS(ES)	10. SPONSOR/MONITOR'S ACRONYM(S)
	11. SPONSOR/MONITOR'S REPORT NUMBER(S)

12. DISTRIBUTION/AVAILABILITY STATEMENT

Approved for public release; distribution unlimited.

13. SUPPLEMENTARY NOTES

14. ABSTRACT

A detection system for theophylline that combined the recognition properties of an aptamer and that plasmonic response of gold nanoparticles (AuNPs) is presented. The aptamer was used as a linker for AuNPs functionalized with complementary sequences to the aptamer (DNA-AuNPs), producing supramolecular complexes that disassemble when exposed to theophylline due to aptamer binding. The detection event was reported as a change in the AuNPs plasmonic peak and intensity. Addition of a spacer on the DNA immobilized on the AuNPs facing the aptamer binding site improved the aggregates? response, doubling the detection range of system response to theophylline. Modification of the oligonucleotides immobilized on the AuNPs that reduced the interparticle distance in the aggregated state suppressed their response to theophylline and addition of the spacer recovered it. This work demonstrated that the design of oligonucleotides immobilized on the AuNPs could be used to improve their plasmonic response without affecting aptamer performance.

15. SUBJECT TERMS

16. SECURITY CLASSIFICATION OF:			17. LIMITATION OF ABSTRACT	18. NUMBER OF PAGES	19a. NAME OF RESPONSIBLE PERSON
a. REPORT	b. ABSTRACT	c. THIS PAGE			
unclassified	**unclassified**	**unclassified**		**7**	

Biosensors and Bioelectronics 26 (2010) 23–28

Contents lists available at ScienceDirect

Biosensors and Bioelectronics

journal homepage: www.elsevier.com/locate/bios

Theophylline detection using an aptamer and DNA–gold nanoparticle conjugates

Jorge L. Chávez, Wanda Lyon, Nancy Kelley-Loughnane, Morley O. Stone *

Applied Biotechnology Branch, Human Effectiveness Directorate, Air Force Research Laboratory, Wright-Patterson Air Force Base, OH 45433, USA

ARTICLE INFO

Article history:
Received 19 March 2010
Received in revised form 27 April 2010
Accepted 30 April 2010
Available online 7 May 2010

Keywords:
Gold nanoparticles
Aptamer
Theophylline
Colorimetric
Spacer effect

ABSTRACT

A detection system for theophylline that combined the recognition properties of an aptamer and the plasmonic response of gold nanoparticles (AuNPs) is presented. The aptamer was used as a linker for AuNPs functionalized with complementary sequences to the aptamer (DNA–AuNPs), producing supramolecular complexes that disassemble when exposed to theophylline due to aptamer binding. The detection event was reported as a change in the AuNPs plasmonic peak and intensity. Addition of a spacer on the DNA immobilized on the AuNPs facing the aptamer binding site improved the aggregates' response, doubling the detection range of system response to theophylline. Modification of the oligonucleotides immobilized on the AuNPs that reduced the interparticle distance in the aggregated state suppressed their response to theophylline and addition of the spacer recovered it. This work demonstrated that the design of oligonucleotides immobilized on the AuNPs could be used to improve their plasmonic response without affecting aptamer performance.

Published by Elsevier B.V.

1. Introduction

Hybrid materials formed by the combination of metal nanoparticles and biomolecules have been demonstrated as an efficient way to produce nanostructured materials that can respond to a specific stimulus with a particular signal (Katz and Willner, 2004; Liu and Lu, 2007). Gold nanoparticles have emerged as one of the most exciting probes for the design of nanoparticle-based sensors, mostly due to their colorimetric response to events that affect their surface plasmon resonance. Typically, 13 nm AuNPs are used due to the high reproducibility of their synthesis and well established methods for DNA immobilization on their surface. Two groups reported simultaneously the coupling of AuNPs with oligonucleotides as a means to control the assembly of DNA–AuNPs (Mirkin et al., 1996; Alivasatos et al., 1996). The red AuNP suspensions formed purple aggregates after hybridization due to a reduction in the interparticle distance. Heating the DNA-linked AuNP suspensions promoted the controlled disassembly of the nanoparticle aggregates, observed as a change in color from purple (aggregated) to red (dispersed) (Elghanian et al., 1997). Moreover, this process was observed to be reversible—upon cooling, the aggregates reformed and upon heating they separated (Mirkin et al., 1996).

When aptamers are used to link DNA–AuNPs, control over the interparticle distance can be accomplished by the presence of a specific target (Liu and Lu, 2003; Huang et al., 2005). Aptamers are DNA or RNA sequences that bind a specific analyte with affinities and selectivities that rival that of antibodies (Jayasena, 1999). Additional advantages over antibodies are their ease of synthesis and stability against pH, temperature and high ionic strength. They are commonly obtained by the SELEX process, pioneered by Ellington and Szostack (1990) and Tuerk and Gold (1990). Typically, analyte binding involves adoption of a thermodynamically favored conformation that maximizes interaction between the aptamer and the target. Recently, Liu and Lu have used this conformational change upon binding to control the disassembly of DNA–AuNPs under mild conditions (Liu and Lu, 2006a,b). Two sets of DNA–AuNPs were used with an aptamer for adenosine to form sensing aggregates. These purple aggregates disassembled when exposed to adenosine, which was observed as a red-shifted color change (Liu and Lu, 2007).

Here, we report the first use of a nanoparticle-based detection system for theophylline. Theophylline is used as a bronchodilator in cases of asthma, bronchitis and emphysema, having as a drawback its low therapeutic index (Hendeles and Weinberger, 1983). Due to its toxicity, different approaches for monitoring levels of this drug have been proposed. Sekella et al. (2002) showed the use of aptamers for theophylline detection, adapting an idea proposed by Soukup and Breaker (1999). In their approach, a pair of dyes was used to monitor the activity of a ribozyme upon theophylline binding through FRET. Ferapontova et al. (2007) reported the use of an RNA aptamer for electrochemical detection of theophylline, which was subsequently improved to work in serum (Ferapontova et al., 2008; Ferapontova and Gothelf, 2009). Moreover, the use of aptamers on theophylline detection has been shown to be possible on cell-based sensing approaches through

* Corresponding author. Tel.: +1 937 255 8222; fax: +1 937 656 5448.
E-mail address: Morley.Stone@wpafb.af.mil (M.O. Stone).

0956-5663/$ – see front matter. Published by Elsevier B.V.
doi:10.1016/j.bios.2010.04.049

Table 1
Oligonucleotide sequences used in this study.

Name	Sequence
DNA1	5′-TCACAGATGAGTAAAAAAAAAAAA-$(CH_2)_3$-SH-3′
DNA2	5′-HS-$(CH_2)_6$-TCGCCTTAGA-3′
PolyA-DNA2	5′-HS-$(CH_2)_6$-AAAAAAAAAA TCGCCTTAGA-3′
DNA3	5′-CTCATCTGTGATCTAAGGCGAUACCAGCCGAAAGGCCC UUGGCAGCGUC-3′
t-DNA3	5′-HS-$(CH_2)_6$-TCTAAGGCGAUACCAGCCGAAAGGCCCUU GGCAGCGUC-3′

the use of riboswitches (Harbaugh et al., 2009). The goal of this work was to design a fast and easy-to-read detection system that responded to therapeutically relevant theophylline concentrations. Our first approach was based on the strategy reported by Liu and Lu (2006a), using DNA–AuNPs containing oligonucleotides complementary to an aptamer for theophylline. Subsequently, we varied the interparticle distance in the aggregated state and sterics around the aptamer binding site and studied the effect of this modification on aptamer binding and the AuNPs plasmonic response.

2. Experimental

2.1. Materials

Sodium citrate, sodium chloride, tris(hydroxymethyl)aminomethane (tris), tris acetate, $HAuCl_4$, theophylline and caffeine were purchased from Sigma–Aldrich (St. Louis, MO). Gold nanoparticles (15 nm hydrodynamic diameter) were synthesized by reduction of $HAuCl_4$ with sodium citrate following procedures from the literature (Liu and Lu, 2008). Oligonucleotides were purchased from Integrated DNA Technologies (Coralville, IA) and dissolved in 10 mM tris buffer (pH 7.4). DNA sequences used are shown in Table 1, sequences DNA1, DNA2 and polyA-DNA2 were purified by standard desalting. The aptamer sequence (DNA3) and the thiolated aptamer sequence (t-DNA3) were a hybrid composed of a mixture of deoxy- and ribonucleic acids adapted from the literature (Zimmerman et al., 1997) and purified by polyacrylamide gel electrophoresis. The binding pocket of DNA3 and t-DNA3 was made of RNA bases. The non-binding portion was made of deoxyribonucleic acids to increase the stability of the oligonucleotide.

2.2. Preparation of DNA–AuNPs and nanoparticle aggregates

The AuNPs (3 mL, 10 nM, Millipore water) were mixed with the thiolated oligonucleotides dissolved in tris buffer at pH 7.4 (13.5 μL, 1 mM for DNA 1, 2 and polyA2; and 45 μL, 200 μM for t-DNA3). The mixtures were left in the dark overnight to allow for chemisorption of the thiol groups on the surface of the AuNPs. Subsequently, tris acetate buffer and NaCl were added to obtain a final concentration of 5 and 100 mM, respectively, and, stored again in the dark overnight. The DNA–AuNPs were centrifuged twice at 16 000 × *g* for 12 min to remove unbound oligonucleotides and resuspended in 25 mM tris acetate buffer containing 100 mM NaCl. A final centrifugation was performed followed by resuspension in hybridization buffer (see below). The 3-piece and 3-piece-polyA aggregates were obtained by mixing equimolar volumes of the DNA–AuNPs, as determined by their UV–vis extinction at 520 nm (typically 600 μL each, 13.5 nM), with the free aptamer (DNA3, 18 μL, 10 μM) in hybridization buffer: 300 mM NaCl, 25 mM tris acetate, pH 8.2 and stored at 4 °C. The color of the suspensions changed after a few hours from red to purple, and aggregates were obtained after overnight hybridization. The aggregates were separated from free aptamer by centrifugation at 800 × *g* for 1.5 min and resuspended in fresh hybridization buffer (AuNP ~45 nM). The 2-piece aggregates were obtained by mixing equimolar volumes of the aptamer-coated AuNPs (t-DNA3–AuNPs) and DNA2–AuNPs in 25 mM tris acetate buffer containing 1.5 M NaCl at pH 8.2, overnight. The 2-piece-polyA aggregates were obtained in a similar way and incubated in 25 mM tris acetate buffer containing 1 M NaCl at pH 8.2, overnight. The purification of the aggregates was performed in the same way as for the 3-piece.

2.3. Analyte detection

Analyte detection was started by equilibrating 100 μL of the aggregate suspensions (AuNP ~10 nM) at the temperature of detection for 15 min. Typically, during the first 10 min a slight change in the absorption maxima and its intensity was observed. Subsequently, a certain volume of a stock solution of the analyte was added and the extinction of the mixture measured after 2 min. This process was repeated for each analyte concentration tested in an experiment. Typically, the analyte was added until changes in the absorption maxima were no longer observed. The concentrations reported are from the stock solutions.

3. Results and discussion

3.1. 3-Piece nanoparticle aggregates designs

The aptamer-linked AuNP sensing aggregates were designed based on the work of Liu and Lu (2006a,b). The DNA–AuNPs were obtained by chemisorption of the thiolated oligonucleotides on the surface of the AuNPs (Hurst et al., 2006). The first set of particles (DNA1–AuNPs) was coated with a sequence containing 11 bases complementary to the 5′-end of the aptamer (Table 1). The second set, DNA2–AuNPs, contained 10 bases complementary to the subsequent bases on the aptamer, from which five were involved in the conformational change that occurred during binding (see Fig. S1). The 3-piece aggregates were obtained through hybridization of the complementary sequences in the two sets of DNA–AuNPs and the aptamer in buffer supplemented with 300 mM NaCl, since lower salt concentrations resulted in incomplete hybridization. As shown in Fig. 1 and Fig. S1, the nanoparticle aggregates formed with the DNA2–AuNPs facing the aptamer sequence involved in binding. The aptamer conformational change necessary to accommodate theophylline required the formation of a stem that involved five bases formerly hybridized to the DNA2–AuNPs (see Fig. S1). The five bases left hybridized after binding could not maintain the aggregated state under the detection conditions (Liu and Lu, 2006a), and resulted in the aggregates' disassembly, as observed colorimetrically by the AuNPs.

The use of minor modifications in the sequence of the oligonucleotides coating the AuNPs has been shown to influence the DNA-linked nanoparticles response under different conditions (Liu and Lu, 2007; Jin et al., 2003; Hurst et al., 2006). On the base of this, a 10 adenine spacer (polyA) was added between the thiol group and the sequence complementary to the aptamer in the AuNPs facing the aptamer binding site (DNA2–AuNPs) in the aggregates (see Fig. 1). The aggregates (3-piece-polyA) were formed under the same conditions as the 3-piece system. Addition of the polyA was expected to affect their response to theophylline since it increased the interparticle distance in the aggregates, thus reducing the repulsion between the particles (Jin et al., 2003; Hurst et al., 2006). Moreover, addition of the spacer placed the sequence intended to hybridize with the aptamer further away from the surface, releasing some of the steric constraints around the aptamer binding site and preventing potential interactions between the oligonucleotides and the AuNPs.

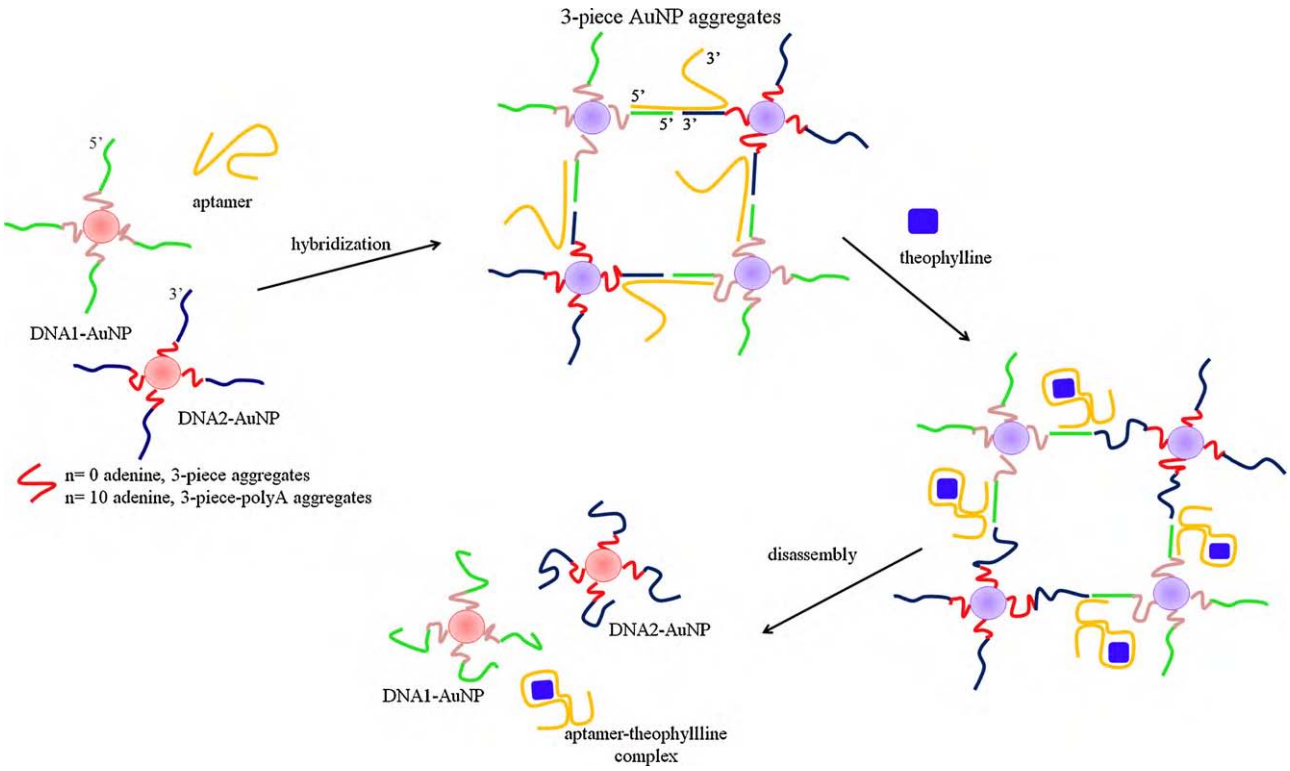

Fig. 1. Representation of the formation of the 3-piece nanoparticle aggregate designs and their disassociation upon exposure to theophylline.

3.2. Theophylline detection with the 3-piece designs: effect of the polyA spacer

Our preliminary studies suggested that the aggregates could respond to theophylline at different temperatures and NaCl concentrations with minimal response to caffeine. Fig. 2a shows the aggregates' response to theophylline at 29 °C in detection buffer: 25 mM tris acetate, 135 mM NaCl, pH 8.2. The aptamer-linked AuNPs responded to theophylline from 50 to 240 μM, covering the therapeutically relevant theophylline concentration range. Their aggregates extinction intensity increased by approx. 70% when exposed to 240 μM theophylline, but responded minimally to caffeine (see inset in Fig. 2a). The chemical structure of caffeine differs from theophylline only by the presence of a methyl group (Fig. 2b), which produced a decrease in the affinity of an RNA aptamer to caffeine by a factor of approximately 10 000 compared to theophylline (Jenison et al., 1994).

The response of the sensing aggregates was quantified using their corrected extinction, defined as the ratio of the extinction at the maxima and at 700 nm. This ratio has been used by others to quantify changes in the aggregated state of AuNPs. This calculation corresponds to well-dispersed AuNPs that show a high extinction at 520 nm and low values at 700 nm, whereas aggregated AuNPs show higher extinction values at 700 nm (Liu and Lu, 2006a,b). Fig. 2c shows that, overall, a linear response to theophylline was observed. This linear dependence differed from similar systems based on aptamers for cocaine and adenosine (Liu and Lu, 2006a). It is known that, due to the cooperativity of the interactions of the DNA–AuNP in the aggregates, the dehybridization of an oligonucleotide linking the AuNPs affects the surrounding

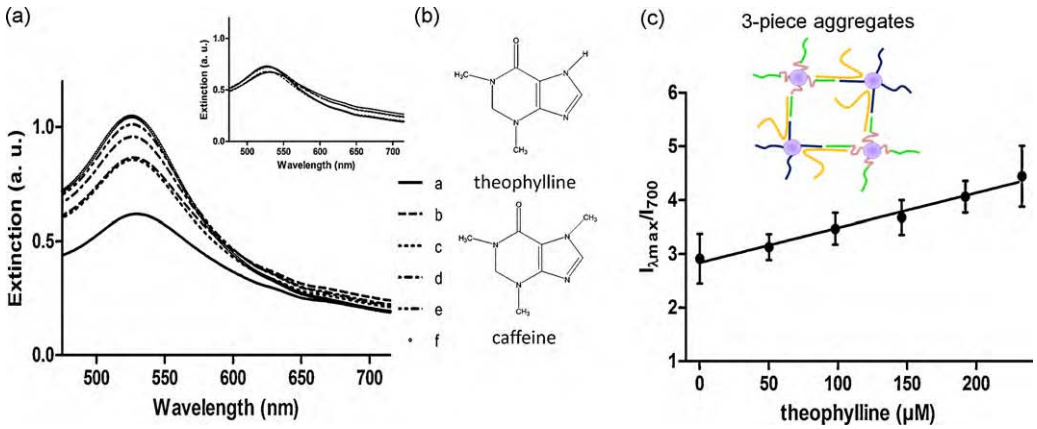

Fig. 2. (a) UV–vis extinction spectra of 3-piece aggregates exposed to theophylline in 25 mM tris acetate buffer containing 135 mM NaCl at 29 °C, pH 8.2; a: 0 μM, b: 50 μM, c: 100 μM, d: 150 μM, e: 190, f: 240 μM. The inset shows their extinction when exposed to caffeine in the same concentration range, (b) chemical structures of theophylline and caffeine and (c) corrected extinction of 3-piece aggregates exposed to theophylline under same conditions as in (a). The error bars represent the standard deviation of measurements taken in three independent experiments.

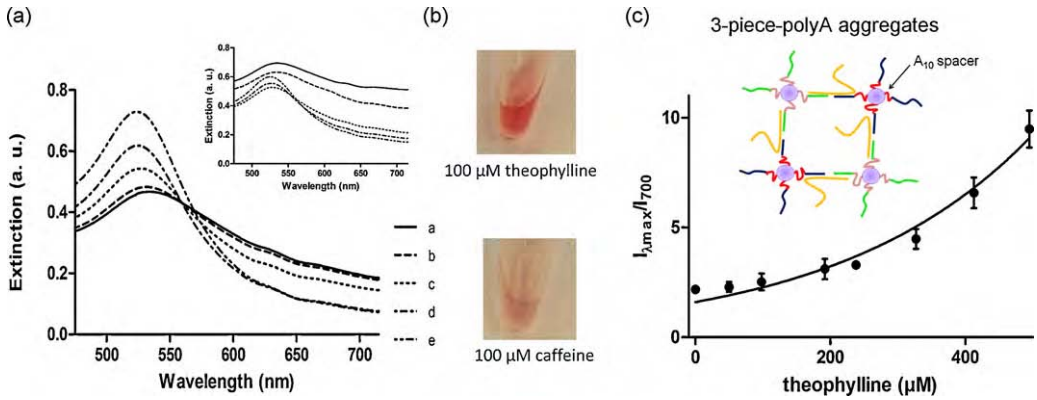

Fig. 3. (a) UV–vis extinction spectra of 3-piece-polyA aggregates exposed to theophylline in 25 mM tris acetate buffer containing 75 mM NaCl at 41 °C, pH 8.2; a: 0, b: 50, c: 240, d: 410, e: 500. The inset shows their extinction when exposed to caffeine, (b) colorimetric response of the 3-piece-polyA aggregates to theophylline and caffeine, and (c) corrected extinction of 3-piece-polyA aggregates exposed to theophylline in 25 mM tris acetate under same conditions as in (a). The error bars represent the standard deviation of measurements taken in three independent experiments. Notice that not all the scans used to obtain the plot are shown for clarity.

aptamer units. For instance, heating the nanoparticle aggregates close to their melting temperature (Tm) releases a small number of oligonucleotides with its associated counterions (Jin et al., 2003). As a consequence, the local salt concentration on the surface of the AuNPs decreases, increasing the interparticle repulsion. After a certain number of dehybridization events have occurred, the nanoparticle aggregates collapse in a very narrow temperature range, showing a sharp melting curve (Jin et al., 2003). A similar cooperative effect was observed by Liu and Lu with their sensing aggregates during analyte detection. This was observed as a linear response of the corrected extinction with a small slope at lower target concentrations (release of the first aptamer units) and a sudden increase in the slope after a certain critical target concentration was reached (collapse of the aggregates, increase in extinction intensity). In our case, when the aggregates were tested at 28 °C, only a change in the extinction maxima was observed upon theophylline addition with a mild change in its intensity (aptamer release only, see Fig. S2 in the Supporting Information). This seemed to indicate that, at this temperature, despite theophylline binding and aptamer release, the AuNP aggregates could not be broken apart completely. Raising the detection temperature to 29 °C did promote an increase in the absorption intensity of 70% upon addition of the target (disassembly of the aggregates) as shown in Fig. 2a. However, at this temperature, the release of the first aptamer units has been promoted before addition of the target. As a consequence, not a "two-step" but a linear response was obtained, which corresponded to the aggregates' collapse only. Increasing the temperature to 30 °C, produced the disassembly of the aggregates without addition of the target, since this temperature was too close to the Tm. We believe the reason for the lack of a "two step" response with our system is related to differences in the steric and geometric requirements for aptamer folding during binding. To test this hypothesis, we placed a 10 adenine spacer (polyA) in the DNA2–AuNPs sequence to increase the interparticle distance and release some of the steric constraints the aptamer may experience in the aggregated particles.

As shown in Fig. 3a, the 3-piece-polyA aggregates responded with a 56% increase in its extinction coefficient when exposed to 500 μM theophylline at 41 °C in tris acetate buffer containing 75 mM NaCl. Under the same conditions a minimal response to caffeine was observed in the same concentration range, showing an improvement in suppressing false positives compared to the 3-piece system (see inset in Fig. 3a). The disassembly of the aggregates could be followed qualitatively by the naked-eye, as shown in Fig. 3b. Quantification of the colorimetric changes showed that the response can be fitted to an exponential growth curve (Fig. 3c). To confirm these results were the typical response of the system and not unique to these conditions, we tested the 3-piece-polyA aggregates at different salt concentrations and temperatures. Fig. S3 in the Supporting Information shows the response of the system in buffer containing 100 mM NaCl at 43 °C, where it can be observed that the aggregates showed an exponential growth-like response to theophylline with minimal response to caffeine. This type of response is in agreement with the cooperativity of the interparticle interactions in the aggregated state. Lu and Liu reported that aggregates formed with a spacer in the DNA2–AuNPs and aptamers for cocaine and adenosine, completely lost the ability to respond to their targets when the spacer contained three or more adenines. The suppression of the aggregates' response when the spacer was used was attributed by the authors to thermodynamic factors favoring the aggregated state (Liu and Lu, 2007). In their design, the energy difference in between the aptamer hybridized with AuNPs and binding its target was not enough to promote the binding event and the corresponding disassociation of the nanoparticle aggregates. Interestingly, in our case, the spacer produced an improvement in the aggregates response. The RNA aptamer for theophylline has a Kd of approximately 350 nM (Jenison et al., 1994), significantly lower than the ones for adenosine and cocaine, which would make folding upon target binding more thermodynamically favored.

The difference in the response of our 3-piece and 3-piece-polyA systems can be explained by the following reasons: (i) the 3-piece-polyA system with a larger interparticle distance and reduced interparticle repulsion, could discriminate better between chemical analogs; the shorter interparticle distance in the 3-piece design may produce a higher energy system that breaks apart with molecules that resemble theophylline at lower concentrations and (ii) the polyA spacer may release some of the steric constraints around the binding site, allowing for better conditions for aptamer folding and binding in the aggregated state. To test these ideas, a new system was designed to separate each of these effects, as explained in Section 3.3.

3.3. 2-Piece nanoparticle aggregates designs

The effects observed by addition of a spacer on the DNA2–AuNPs seemed to be a combination of modifying the interparticle distance and the sterics around the aptamer binding site. In order to separate these two effects, a 2-piece AuNPs aggregate system was designed based on the 3-piece system. The aptamer sequence was modified by deleting its 5′-end used for hybridization with the DNA1–AuNPs and the addition of a thiol moiety to its new 5′-end. The t-DNA3–AuNPs were obtained by chemisorption of the aptamer. The 2-piece aggregates were formed by hybridizing the

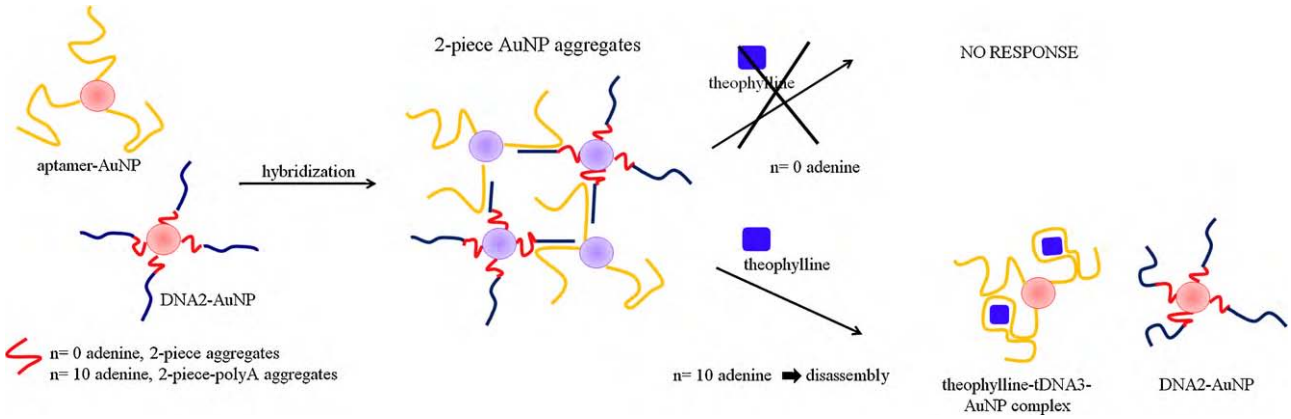

Fig. 4. Representation of the formation of the 2-piece nanoparticle aggregate designs and response to theophylline.

t-DNA3–AuNPs and DNA2–AuNPs in buffer containing 1.5 M NaCl (Fig. 4). The higher NaCl concentration compared to the 3-piece system, was necessary due to the need to bring the AuNPs closer for hybridization, which required a better screening of the AuNP surface charges. The interparticle distance in the 2-piece aggregates was reduced to approximately half the separation in the 3-piece system, to evaluate the effect of the interparticle distance alone, on their response to theophylline. The effect of the spacer was evaluated using the corresponding 2-piece-polyA aggregates, which were obtained by hybridizing the t-DNA3–AuNPs and polyA-DNA2–AuNPs.

3.4. Theophylline detection with the 2-piece aggregates: effects of the polyA spacer

Due to the high NaCl concentration needed for hybridization, the lowest salt concentration that could be used to prevent the 2-piece aggregates from breaking at room temperature was 700 mM. This system failed to respond to theophylline at different salt concentrations (above 700 mM) and temperatures. Even exposure to theophylline concentrations well above the ones needed to observe a response with the 3-piece systems (up to 6000 μM) failed to promote breaking of the aggregates. This lack of response could be due to stronger interparticle attractive forces that emerge at such short interparticle distances, which would prevent the aptamer from binding. Even if binding of the analyte and dehybridization occurred, breaking of the nanoparticle aggregates could be suppressed by such interactions. It may be argued that the high salt concentration used in these studies could inhibit aptamer binding by stabilization of double-stranded DNA, which may prevent the aptamer conformational change needed for binding. This cannot be ruled out, however it is unlikely in this case, since the selection process used to discover the RNA version of this aptamer involved working with a buffer containing 500 mM NaCl (Jenison et al., 1994).

Addition of the spacer in the 2-piece system surprisingly recovered the ability of the aggregates to respond to theophylline. The 2-piece-polyA aggregates did not show any response when exposed to theophylline below 500 μM, but a significant increase in their extinction intensity was observed at concentrations above 1000 μM and up to approx. 2000 μM, in tris acetate buffer containing 250 mM NaCl, pH 8.2 at 43 °C (Fig. 5a). Similar to the previous systems studied, the aggregates showed a minimal response to caffeine under the same conditions (inset in Fig. 5a). Interestingly, the target concentrations necessary to observe a response were significantly higher than the 3-piece designs. As discussed in Section 3.3, we believe the spacer is releasing some of the steric constraints around the aptamer binding site, which allows enough space to adopt the optimal conformation for binding. The need for higher target concentrations to promote the aggregate disassembly is not surprising since it can be anticipated that more binding events will be necessary to overcome the strong attractive forces holding the particles together in this design. This system responded in an exponential growth-like manner to theophylline, similar to the 3-piece-polyA system (Fig. 5b). These results were confirmed by evaluating their response in buffer containing 350 mM NaCl (Fig. S4 in the Supplementary Information). The fact that the addition of the spacer recovered the ability of the aggregates to

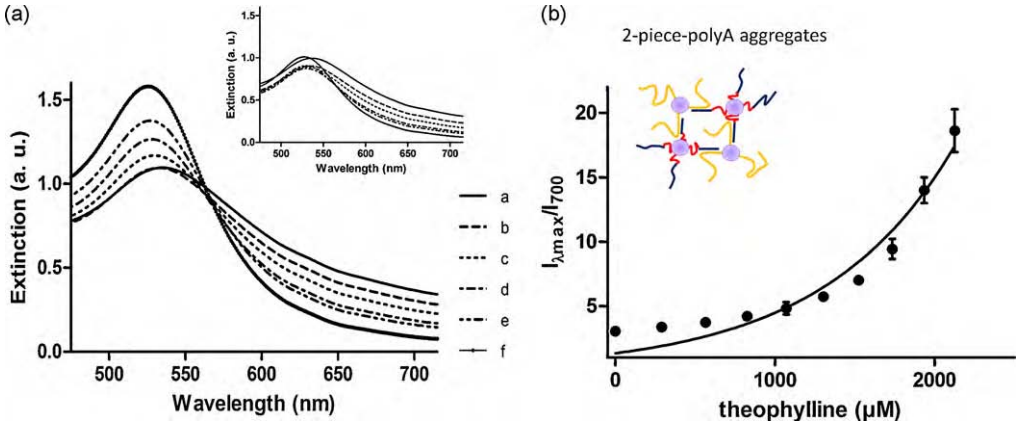

Fig. 5. (a) UV–vis extinction spectra of 2-piece-polyA aggregates exposed to theophylline in 25 mM tris acetate buffer containing 250 mM NaCl at 43 °C, pH 8.2; a: 0 μM, b: 570 μM, c: 1070 μM, d: 1530 μM, e: 1740 μM, f: 2130 μM. The inset shows their extinction when exposed to caffeine and (b) corrected extinction of 2-piece-polyA aggregates exposed to theophylline under the same conditions as in (a). The error bars represent the standard deviation of measurements taken in three independent experiments.

disassemble when exposed to theophylline indicated that tuning the degree of steric constraints around the aptamer binding site is extremely important and can affect dramatically the outcome of the design of sensors based on aptamer and nanoparticles.

4. Conclusions

A nanoparticle-based detection system for theophylline was designed for the first time using an aptamer as a recognition motif and gold nanoparticles as colorimetric reporters. A 3-piece system was designed with two sets of DNA-coated AuNPs and an aptamer specific to theophylline. This system showed a linear response to theophylline over a concentration range that covered therapeutically relevant theophylline levels without response to caffeine. Addition of a 10 adenine spacer to the DNA at the nucleic acid/nanoparticle interface facing the aptamer binding sequence resulted in an improve system able to respond to a broader theophylline concentration range. Moreover, the 3-piece polyA aggregates did not respond linearly to theophylline, rather an exponential growth-like response curve was observed. We hypothesized that the spacer released some steric constraints affecting the aptamer in the aggregated state, improving the assay performance. We tested this hypothesis by designing a 2-piece system using AuNPs coated with the aptamer to obtain the sensing aggregates. It was observed that reduction of the interparticle distance suppressed the aggregates' response to theophylline. Addition of the spacer recovered the aptamer activity and AuNPs plasmonic response to theophylline. These results suggested that the spacer placed close to the aptamer/AuNP interface reduced the steric constraints around the aptamer binding site, thus providing favorable conditions for the aptamer conformational change necessary for binding. This work showed that the balance between the interparticle interactions and the aptamer geometric and steric requirements for binding play a crucial role in the nanoparticle aggregate response.

Acknowledgements

This work was funded by the Air Force Office of Scientific Research. JLC participation was supported in part by an appointment to the Postgraduate Research Participation Program at the U.S. Air Force Research Laboratory administered by the Oak Ridge Institute for Science and Education through an interagency agreement between the U.S. Department of Energy and USAFRL.

Appendix A. Supplementary data

Supplementary data associated with this article can be found, in the online version, at doi:10.1016/j.bios.2010.04.049.

References

Alivasatos, A.P., Johnsson, K.P., Peng, X., Wilson, T.E., Loweth, C.J., Bruchez Jr., M.P., Schultz, P.G., 1996. Nature 382, 609–611.
Elghanian, R., Storhoff, J.J., Mucic, R.C., Letsinger, R.L., Mirkin, C.A., 1997. Science 277, 1078–1081.
Ellington, A.D., Szostack, J.W., 1990. Nature 346, 818–822.
Ferapontova, E.E., Shipovskov, S., Gorton, L., 2007. Biosens. Bioelectron. 22, 2508–2515.
Ferapontova, E.E., Olsen, E.M., Gothelf, K.V., 2008. J. Am. Chem. Soc. 130, 4256–4258.
Ferapontova, E.E., Gothelf, K.V., 2009. Langmuir 25, 4279–4283.
Harbaugh, S., Kelley-Loughnane, N., Davidson, M., Narayanan, L., Trott, S., Chushak, Y., Stone, M.O., 2009. Biomacromolecules 10, 1055–1060.
Hendeles, L., Weinberger, M., 1983. Pharmacotherapy 3 (1), 2–44.
Huang, C.-C., Huang, Y.-F., Cao, Z., Tan, W., Chang, H.-T., 2005. Anal. Chem. 77, 5735–5741.
Hurst, S.J., Lytton-Jean, A.K.R., Mirkin, C.A., 2006. Anal. Chem. 78, 8313–8318.
Jayasena, S.D., 1999. Clin. Chem. 45, 1628–1650.
Jenison, R.D., Gill, S.C., Pardi, A., Polisky, B., 1994. Science 263, 1425–1429.
Jin, R., Wu, G., Li, Z., Mirkin, C.A., Schatz, G.C., 2003. J. Am. Chem. Soc. 125, 1643–1654.
Katz, E., Willner, I., 2004. Angew. Chem. Int. Ed. 43, 6042–6108.
Liu, J., Lu, Y., 2003. J. Am. Chem. Soc. 125, 6642–6643.
Liu, J., Lu, Y., 2006a. Angew. Chem. Int. Ed. 45, 90–94.
Liu, J., Lu, Y., 2006b. Adv. Mater. 18, 1667–1671.
Liu, J., Lu, Y., 2007. J. Am. Chem. Soc. 129, 8634–8643.
Liu, J., Lu, Y., 2008. Nat. Protocols 1, 246–252.
Mirkin, C.A., Letsinger, R.L., Mucic, R.C., Storhoff, J.J., 1996. Nature 382, 607–609.
Sekella, P.T., Rueda, D., Walter, N.G., 2002. RNA 8, 1242–1252.
Soukup, G.A., Breaker, R.R., 1999. Proc. Natl. Acad. Sci. 96, 3584–3589.
Tuerk, C., Gold, L., 1990. Science 249, 505–510.
Zimmerman, G.R., Jenison, R.D., Wick, C.L., Simorre, J.-P., Pardi, A., 1997. Nat. Struct. Biol. 4, 644–649.